

## A simple recipe for estimating atmospheric stability solely based on surface-layer wind speed profile

Basu, Sukanta

**DOI**

[10.1002/we.2203](https://doi.org/10.1002/we.2203)

**Publication date**

2018

**Document Version**

Final published version

**Published in**

Wind Energy

**Citation (APA)**

Basu, S. (2018). A simple recipe for estimating atmospheric stability solely based on surface-layer wind speed profile. *Wind Energy*, 21(10), 937-941. <https://doi.org/10.1002/we.2203>

**Important note**

To cite this publication, please use the final published version (if applicable). Please check the document version above.

**Copyright**

Other than for strictly personal use, it is not permitted to download, forward or distribute the text or part of it, without the consent of the author(s) and/or copyright holder(s), unless the work is under an open content license such as Creative Commons.

**Takedown policy**

Please contact us and provide details if you believe this document breaches copyrights. We will remove access to the work immediately and investigate your claim.

SHORT COMMUNICATION

# A simple recipe for estimating atmospheric stability solely based on surface-layer wind speed profile

Sukanta Basu 

Faculty of Civil Engineering and Geosciences,  
Delft University of Technology, Delft, The  
Netherlands

**Correspondence**

Sukanta Basu, Faculty of Civil Engineering and  
Geosciences, Delft University of Technology,  
Stevinweg 1, 2628 CN Delft, The Netherlands.  
Email: s.basu@tudelft.nl

## Abstract

The wind energy community is gradually recognizing the significance of atmospheric stability in both power production and structural loading. However, estimating stability requires temperature gradient data which are not commonly measured by the wind farm developers or operators. To circumvent this problem, we propose a simple approach *à la* Swinbank, to estimate stability from only 3 levels of wind speed measurements. As such, this approach is ideally suited for sodar- and lidar-based wind measurements owing to their high vertical resolution in the surface layer.

## KEYWORDS

extrapolation, gradient method, Obukhov length, profile method, similarity theory

The Monin-Obukhov similarity theory (MOST)<sup>1</sup> -based surface-layer wind speed profile equation can be written as<sup>2</sup>

$$U(z) = \frac{u_*}{k} \left[ \ln \left( \frac{z}{z_o} \right) - \psi_m \left( \frac{z}{L} \right) + \psi_m \left( \frac{z_o}{L} \right) \right], \quad (1)$$

where,  $\psi_m$  is the so-called stability correction term. This equation has 3 unknowns: aerodynamic surface roughness ( $z_o$ ), Obukhov length ( $L$ ), and friction velocity ( $u_*$ ). Traditionally, either the so-called gradient or the profile method is used to estimate these unknowns.<sup>2,3</sup> Once determined, these micro-meteorological variables can be effectively used in conjunction with Equation 1 (or one of its generalized versions<sup>4</sup>) for the vertical extrapolation of wind speeds up to (or higher than) the turbine hub-heights.<sup>5-7</sup>

To the best of our knowledge, with the exception of a multivariate optimization-based approach by Lo,<sup>8</sup> all the other existing gradient or profile methods<sup>2,9</sup> require temperature data from 2 sensor-heights in addition to wind speed measurements. However, in the wind industry, it is not a common practice to measure temperature or temperature gradients. Thus, accurately estimating atmospheric stability, commonly quantified by  $L$ ,<sup>2,5</sup> remains a challenging task in wind resource estimation and other wind energy applications.

With the advent of remote sensing-based wind measuring instruments (eg, sodar and lidar), high vertical resolution ( $\Delta z$  on the order of a few meters) wind profiles are now abundantly available. In this short communication, we document a simple way to estimate  $L$  and other unknowns from Equation 1 with only 3 levels of wind speed measurements; absolutely no temperature information is needed. We call this method the hybrid-wind (or, H-W) approach. We explain this approach in a step-by-step manner so that it can be easily implemented by engineers and practitioners outside academia.

For 3 wind sensor-heights of  $z_1$ ,  $z_2$ , and  $z_3$ , Equation 1 can be rewritten as

$$U(z_1) = \frac{u_*}{k} \left[ \ln \left( \frac{z_1}{z_o} \right) - \psi_m \left( \frac{z_1}{L} \right) + \psi_m \left( \frac{z_o}{L} \right) \right], \quad (2a)$$

$$U(z_2) = \frac{u_*}{k} \left[ \ln \left( \frac{z_2}{z_o} \right) - \psi_m \left( \frac{z_2}{L} \right) + \psi_m \left( \frac{z_o}{L} \right) \right], \quad (2b)$$

$$U(z_3) = \frac{u_*}{k} \left[ \ln \left( \frac{z_3}{z_o} \right) - \psi_m \left( \frac{z_3}{L} \right) + \psi_m \left( \frac{z_o}{L} \right) \right]. \quad (2c)$$

From these equations, the vertical wind speed difference (aka increment) terms can be computed as follows:

$$\Delta U_{21} = U(z_2) - U(z_1) = \frac{u_*}{k} \left[ \ln \left( \frac{z_2}{z_1} \right) - \psi_m \left( \frac{z_2}{L} \right) + \psi_m \left( \frac{z_1}{L} \right) \right], \quad (3a)$$

This is an open access article under the terms of the Creative Commons Attribution License, which permits use, distribution and reproduction in any medium, provided the original work is properly cited.

© 2018 The Authors Wind Energy Published by John Wiley & Sons Ltd.

$$\Delta U_{31} = U(z_3) - U(z_1) = \frac{u_*}{k} \left[ \ln \left( \frac{z_3}{z_1} \right) - \psi_m \left( \frac{z_3}{L} \right) + \psi_m \left( \frac{z_1}{L} \right) \right]. \quad (3b)$$

Finally, a ratio of these differences can be written as

$$R = \frac{\Delta U_{31}}{\Delta U_{21}} = \frac{\ln \left( \frac{z_3}{z_1} \right) - \psi_m \left( \frac{z_3}{L} \right) + \psi_m \left( \frac{z_1}{L} \right)}{\ln \left( \frac{z_2}{z_1} \right) - \psi_m \left( \frac{z_2}{L} \right) + \psi_m \left( \frac{z_1}{L} \right)}. \quad (4)$$

It is needless to point out that  $R$  is a (nonlinear) function of only  $L$ . Thus, if  $R$  varies in a monotonic manner with respect to  $L$ , it will be straightforward to estimate  $L$  from measured  $R$  values via Equation 4.

The behavior of  $R$  depends entirely on the stability correction term ( $\psi_m$ ). For neutral condition (ie,  $\frac{z}{L} = 0$ ),  $\psi_m$  equals to zero. In this case,  $R$  is simply a function of 3 sensor heights:

$$R_N = \frac{\ln \left( \frac{z_3}{z_1} \right)}{\ln \left( \frac{z_2}{z_1} \right)}. \quad (5)$$

Assuming  $z_3 > z_2 > z_1$ , it is trivial to show that  $R_N > 1$ . By using well-accepted  $\psi_m$  functions, it is also not difficult to show that  $R$  is larger (smaller) than  $R_N$  for stable (unstable) conditions.

The most popular  $\psi_m$  functions, attributed to Businger and Dyer,<sup>10-12</sup> are formulated as

$$\psi_m = 2 \ln \left( \frac{1+x}{2} \right) + \ln \left( \frac{1+x^2}{2} \right) - 2 \tan^{-1} x + \frac{\pi}{2}; \quad \text{for } \frac{z}{L} \leq 0, \quad (6a)$$

$$\psi_m = -\frac{5z}{L}; \quad \text{for } \frac{z}{L} \geq 0, \quad (6b)$$

where  $x = \left( 1 - \frac{16z}{L} \right)^{1/4}$ . The variation of  $R$  with respect to  $1/L$  is portrayed in Figure 1. As an illustration, the sensor heights are assumed to be at 5, 10, and 20 m, respectively. For these specific height values,  $R_N = 2$ . Clearly, for unstable conditions (left panel of Figure 1),  $R$  monotonically decreases with increasing instability. In contrast, for stable conditions (right panel of Figure 1),  $R$  shows a monotonically increasing trend with increase in stability.

Given the monotonic behavior of  $R$  with respect to  $1/L$ , as depicted in Figure 1, one can easily estimate  $L$  given any measured value of  $R$ . In this regard, any suitable root finding algorithm (eg, the Levenberg-Marquardt approach) can be used in conjunction with Equation 4. In a nutshell, the proposed H-W approach for stability estimation can be summarized in 3 steps:

1. Compute  $R$  based on measured  $U(z_1)$ ,  $U(z_2)$ , and  $U(z_3)$ .
2. Given  $z_1$ ,  $z_2$ , and  $z_3$ , calculate the value of  $R_N$  using Equation 5.
3. If  $R < R_N$ , then use Equation 4 in conjunction with Equation 6a to estimate  $L$ . Conversely, if  $R > R_N$ , then make use of Equation 6b instead of Equation 6a.

Once Obukhov length ( $L$ ) is estimated, one can estimate the friction velocity ( $u_*$ ) from Equations 3a and 3b. Since there are 2 equations and only one unknown, the conventional linear regression approach with ordinary least squares could be used. Now,  $L$  is defined as

$$L = -\frac{\Theta_o u_*^3}{kg(\overline{w\theta})}, \quad (7)$$

where  $\overline{w\theta}$  is the surface sensible heat flux. The von Kármán constant is denoted by  $k$  ( $k = 0.4$ );  $g$  is the well-known gravitational constant and  $\Theta_o$  is a reference temperature (often assumed to be equal to 300 K). After estimating  $L$  and  $u_*$ , Equation 7 can be inverted to estimate  $\overline{w\theta}$ . In other words, both the turbulent momentum and sensible heat fluxes can be (indirectly) estimated using the H-W approach.

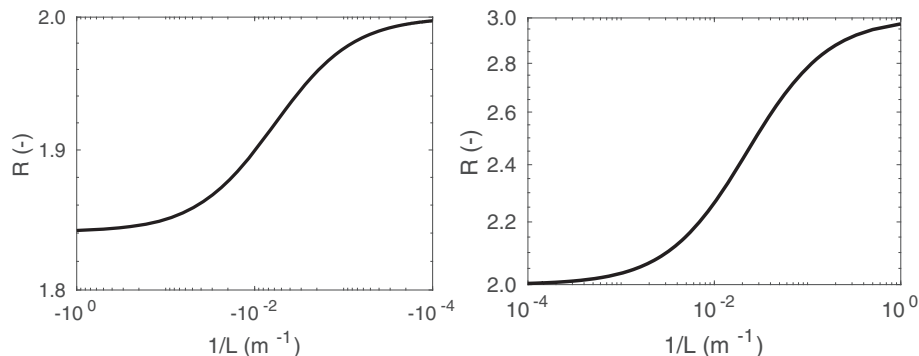


**FIGURE 1** Variation of  $R$  with respect to inverse Obukhov length ( $1/L$ ). The left and right panels represent unstable and stable conditions, respectively. The  $\psi_m$  formulations by Businger and Dyer (ie, Equations 6a and 6b) are used here. In these illustrations,  $z_1, z_2, z_3$  are assumed to be equal to 5, 10, and 20 m, respectively. For near-neutral condition ( $1/L \rightarrow 0$ ),  $R$  asymptotically approaches 2

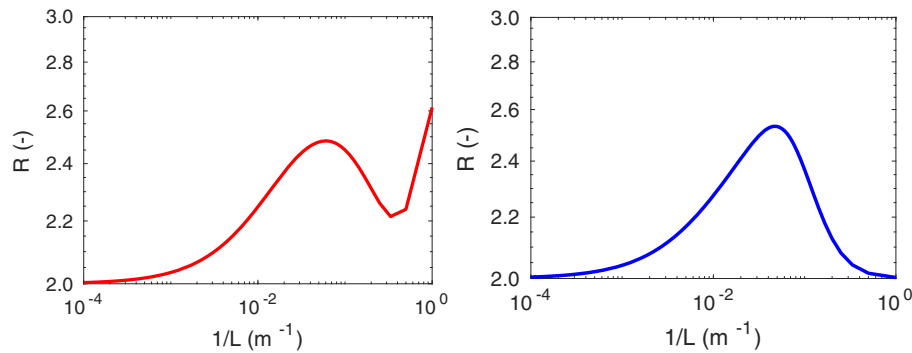


**FIGURE 2** Variation of  $R$  with respect to inverse Obukhov length ( $1/L$ ). The left and right panels represent  $\psi_m$  formulations by Beljaars and Holtslag<sup>13</sup> (Equation 10) and Cheng and Brutsaert<sup>14</sup> (Equation 11), respectively. In these illustrations,  $z_1, z_2, z_3$  are assumed to be equal to 5, 10, and 20 m, respectively [Colour figure can be viewed at [wileyonlinelibrary.com](http://wileyonlinelibrary.com)]

We would like to note that the H-W approach can be further simplified if one has access to reliable aerodynamic roughness value ( $z_o$ ). Under this circumstance, only 2 levels of wind speed data will be required as by definition  $U(z_o) = 0$ . Then, Equations 4 and 5 become, respectively,

$$R_* = \frac{U_3}{U_2} = \frac{\ln\left(\frac{z_3}{z_o}\right) - \psi_m\left(\frac{z_3}{L}\right) + \psi_m\left(\frac{z_o}{L}\right)}{\ln\left(\frac{z_2}{z_o}\right) - \psi_m\left(\frac{z_2}{L}\right) + \psi_m\left(\frac{z_o}{L}\right)}, \quad (8)$$

$$R_{*N} = \frac{\ln\left(\frac{z_3}{z_o}\right)}{\ln\left(\frac{z_2}{z_o}\right)}. \quad (9)$$

The rest of the procedure remains the same as elaborated before.

Before demonstrating the capabilities of the H-W approach, some potential pitfalls regarding its usage should be mentioned. First, MOST<sup>1</sup> is strictly valid in a horizontally homogeneous surface layer (where the Coriolis effects can be neglected). In the surface layer (aka constant flux layer), the turbulent fluxes are assumed to be invariant with height. Thus, all the sensor heights (ie,  $z_1, z_2, z_3$ ) should be within the surface layer to avoid violation of MOST. For strongly stratified conditions, the surface layer could be only a few meters deep; the H-W approach should be avoided under that scenario. Second, the H-W approach implicitly assumes that wind speed values increase with height. If such condition is not met, it should not be used.

Last, we strongly recommend the usage of stability correction functions ( $\psi_m$ ) proposed by Businger and Dyer<sup>10-12</sup> while using the H-W approach. Over the years, several other  $\psi_m$  formulations have been proposed in the literature. Most of these formulations disagree among themselves for moderately and strongly stable conditions; for other stability conditions, the consensus is generally very good. For stable condition, the formulation by Beljaars and Holtslag<sup>13</sup> reads as

$$\psi_m = -a\frac{z}{L} - b\left(\frac{z}{L} - \frac{c}{d}\right)\exp\left(-d\frac{z}{L}\right) - \frac{bc}{d}; \quad \text{for } \frac{z}{L} \geq 0, \quad (10)$$

where  $a = 1, b = \frac{2}{3}, c = 5$ , and  $d = 0.35$ . For the same stability regime, Cheng and Brutsaert<sup>14</sup> proposed

$$\psi_m = -a \ln \left[ \frac{z}{L} + \left( 1 + \left( \frac{z}{L} \right)^b \right)^{\frac{1}{b}} \right]; \quad \text{for } \frac{z}{L} \geq 0, \quad (11)$$

where  $a = 6.1, b = 2.5$ . The  $R$ -vs- $1/L$  plots based on these formulations are shown in Figure 2. In contrast to the Businger-Dyer formulation-based plot (right panel of Figure 1), these plots do not show monotonic behavior (for  $L < 20$  m or so). In other words, multiple roots are possible for a given  $R$  value. As a result,  $L$  cannot be estimated unequivocally.

To validate the H-W approach, we analyze multi-year (2001-2016) meteorological observations measured on the 200-m tall Cabauw tower in the Netherlands.<sup>15</sup> Even though the landscape at Cabauw is quite flat and open (grassland), the existence of wind breaks and scattered villages cause significant disturbances in the near-surface region.<sup>16</sup> Thus, the Cabauw site is not an ideal location to test any approach which relies on MOST. Nonetheless, owing to its high-quality, it has been used in numerous MOST-related publications<sup>9,17,18</sup>; we also follow suit.

Since, at Cabauw, the daytime mixed layer depth is on average significantly lower than 150 m during the winter months (November-January), we exclude data from these months from our analyses. In addition, we discard data from morning (3-9 UTC) and evening (15-21 UTC) transitional periods because surface layer and upper part of the boundary layer often correspond to different stability regimes. We use wind speed data from the lowest 3 sensor levels ( $z = 10, 20$ , and  $40 \text{ m}^*$ ) of the Cabauw tower, to estimate  $R$ . To reduce random errors, we make use of vertical profiles averaged

\* During nighttime, the surface layer is usually shallower than  $z = 40 \text{ m}$ . As such, MOST is not valid at this height for moderately and strongly stratified conditions (categories  $g$  and  $h$ , respectively). Thence, our findings for these categories should be regarded with caution.

over 30 minutes duration. We do not consider cases where wind does not increase monotonically with height; furthermore, we also exclude the weak wind cases (ie,  $U(z) < 1 \text{ m s}^{-1}$ ). After imposing all these constraints, we are left with 84 890 profiles for analyses. Based on Table 1, we classify these profiles into several stability categories. These categories were originally proposed by Holtslag<sup>17</sup> based on Obukhov length. With the aid of Figure 1, we convert them to corresponding ranges of  $R$ .

The median profiles corresponding to each stability class for four key meteorological variables are depicted in Figure 3. These profiles follow clear trends in agreement with the boundary-layer meteorology literature. For example, both wind speed shear and directional shear values increase with increasing stability.<sup>17,19</sup> For stability class  $a$ , the temperature profile closely follows the dry adiabatic lapse rate ( $-9.8 \times 10^{-3} \text{ K m}^{-1}$ ); with increasing stability, the temperature gradients increase monotonically.<sup>2</sup> The decrease in the standard-deviations of horizontal wind speed with increasing stability is also physically realistic.<sup>3</sup> Thus, overall, the proposed H-W approach has the discriminatory power to classify meteorological profiles into appropriate stability classes. In the future, measured turbulent fluxes from different sites will be used to provide more direct validation of the H-W approach.

**TABLE 1** Stability classification

Category	$L$ (m)	$R$ (-)
$a$	$-40 \leq L < -12$	$1.8464 < R \leq 1.8578$
$b$	$-200 \leq L < -40$	$1.8578 < R \leq 1.8994$
$c$	$-1000 \leq L < -200$	$1.8994 < R \leq 1.9583$
$d$	$ L  > 1000$	$1.9583 < R < 2.0673$
$e$	$200 < L \leq 1000$	$2.0673 \leq R < 2.2651$
$f$	$100 < L \leq 200$	$2.2651 \leq R < 2.4191$
$g$	$40 < L \leq 100$	$2.4191 \leq R < 2.6433$
$h$	$10 < L \leq 40$	$2.6433 \leq R < 2.8782$

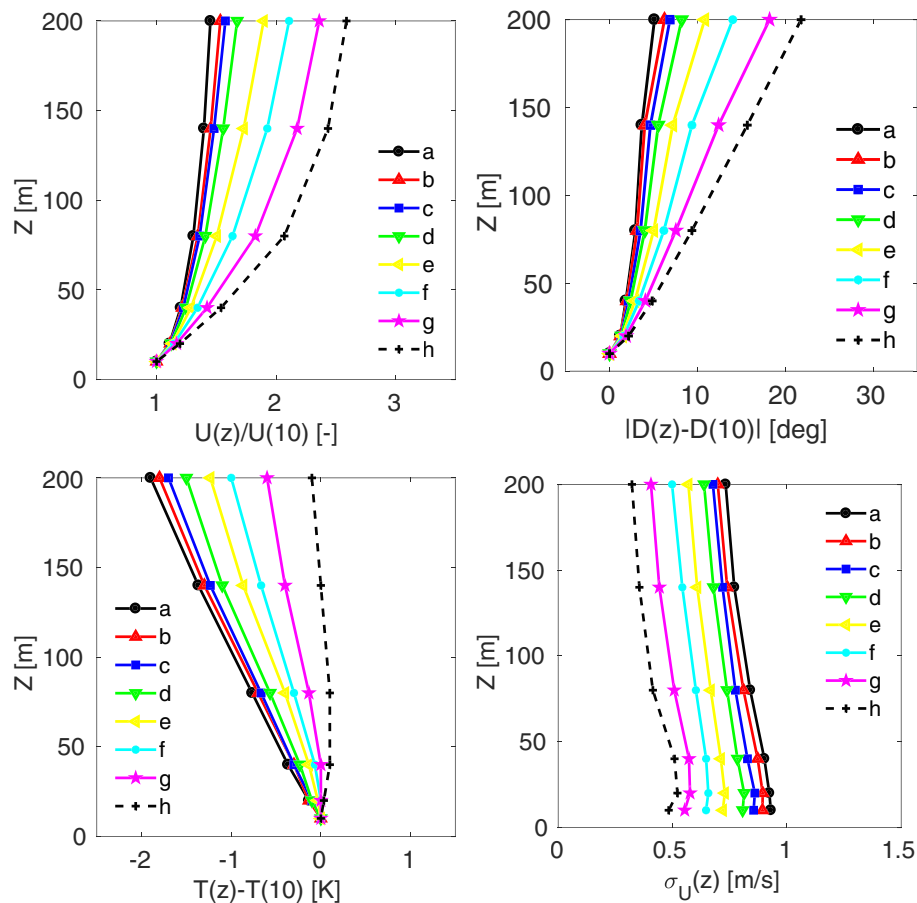


**FIGURE 3** Classification of the Cabauw tower-based meteorological observations. Only the wind speed data from the lowest 3 sensor levels are used to estimate Obukhov length. For each stability class, the median profiles of normalized wind speed (top-left panel), wind directional shear (top-right panel), relative temperature (bottom-left panel), and standard-deviation of horizontal wind speed (bottom-right panel) are shown [Colour figure can be viewed at [wileyonlinelibrary.com](http://wileyonlinelibrary.com)]

Before concluding this article, we would like to call the readers' attention to an old paper by Swinbank.<sup>20</sup> In this work, an “exponential wind profile” with a radically different physical basis than the MOST-based Equation 1 was proposed. In the decade following its publication (as soon as the early 1970s), Swinbank's equation was completely overshadowed by Equation 1 and forgotten by the boundary-layer meteorology community at large. We stumbled upon this paper serendipitously and were surprised to find out that Swinbank<sup>20</sup> outlined an approach virtually identical to the proposed H-W approach, albeit using his “exponential wind profile.” If we are not mistaken, no one else followed-up on his approach or used it in conjunction with Equation 1. The author of the current article has independently “re-invented the wheel” more than half-a-century later.

## ACKNOWLEDGEMENTS

The author is grateful to Pal Arya, Fred Bosveld, Bert Holtslag, Branko Kosović, Avi Lacser, Sethu Raman, and anonymous reviewers for their useful comments. He also thanks the Royal Netherlands Meteorological Institute for providing him access to the Cabauw data sets (CESAR database).

## Conflict of interest

The author declares no potential conflict of interests.

## ORCID

Sukanta Basu  <http://orcid.org/0000-0002-0507-5349>

## REFERENCES

1. Monin AS, Obukhov AM. Basic laws of turbulent mixing in the atmosphere near the ground. *Tr Akad Nauk SSSR Geofiz Inst.* 1954;24:163-187.
2. Arya SP. *Introduction to Micrometeorology*. San Diego, USA: Academic Press; 2001.
3. Emeis S. *Wind Energy Meteorology*. Berlin, Germany: Springer; 2013.
4. Gryning S-E, Batchvarova E, Brümmner B, Jørgensen H, Larsen S. On the extension of the wind profile over homogeneous terrain beyond the surface boundary layer. *Boundary-Layer Meteorol.* 2007;124:251-268.
5. Motta M, Barthelmie RJ, Vølund P. The influence of non-logarithmic wind speed profiles on potential power output at Danish offshore sites. *Wind Energy.* 2005;8:219-236.
6. Sathe A, Gryning S-E, Peña A. Comparison of the atmospheric stability and wind profiles at two wind farm sites over a long marine fetch in the North Sea. *Wind Energy.* 2011;14:767-780.
7. Holtslag MC, Bierbooms WAAM, van Bussel GJW. Extending the diabatic surface layer wind shear profile for offshore wind energy. *Renewable Energy.* 2017;101:96-110.
8. Lo AK. On the determination of boundary-layer parameters using velocity profile as the sole information. *Boundary-Layer Meteorol.* 1979;17:465-484.
9. Nieuwstadt FTM. The computation of the friction velocity  $u_*$  and the temperature scale  $t_*$  from temperature and wind velocity profiles by least-square methods. *Boundary-Layer Meteorol.* 1978;14:235-246.
10. Dyer AJ, Hicks BB. Flux-gradient relationships in the constant flux layer. *Q J R Meteorol Soc.* 1970;96:715-721.
11. Businger JA, Wyngaard JC, Izumi Y, Bradley EF. Flux-profile relationships in the atmospheric boundary layer. *J Atmos Sci.* 1971;28:181-189.
12. Dyer AJ. A review of flux-profile relationships. *Boundary-Layer Meteorol.* 1974;7:363-372.
13. Beljaars ACM, Holtslag AAM. Flux parameterization over land surfaces for atmospheric models. *J Appl Meteorol.* 1991;30:327-341.
14. Cheng Y, Brutsaert W. Flux-profile relationships for wind speed and temperature in the stable atmospheric boundary layer. *Boundary-Layer Meteorol.* 2005;114:519-538.
15. Van Ulden AP, Wieringa J. Atmospheric boundary layer research at Cabauw. *Boundary-Layer Meteorol.* 1996;78:39-69.
16. Verkaik JW, Holtslag AAM. Wind profiles, momentum fluxes and roughness lengths at Cabauw revisited. *Boundary-Layer Meteorol.* 2007;122:701-719.
17. Holtslag AAM. Estimates of diabatic wind speed profiles from near-surface weather observations. *Boundary-Layer Meteorol.* 1984;29:225-250.
18. Optis M, Monahan A, Bosveld FC. Moving beyond Monin–Obukhov similarity theory in modelling wind-speed profiles in the lower atmospheric boundary layer under stable stratification. *Boundary-Layer Meteorol.* 2014;153:497-514.
19. van Ulden AP, Holtslag AAM. Estimation of atmospheric boundary layer parameters for diffusion applications. *J Clim Appl Meteorol.* 1985;24:1196-1207.
20. Swinbank WC. The exponential wind profile. *Q J Roy Meteorol Soc.* 1964;90:119-135.

**How to cite this article:** Basu S. A simple recipe for estimating atmospheric stability solely based on surface-layer wind speed profile. *Wind Energy.* 2018;1–5. <https://doi.org/10.1002/we.2203>